Interface Modification on the Properties of Sisal Fiber-Reinforced Polypropylene Composites

K. L. FUNG, R. K. Y. LI, S. C. TJONG

Department of Physics and Materials Science, City University of Hong Kong, Tat Chee Avenue, Kowloon, Hong Kong, China

Received 1 June 2001; accepted 28 August 2001

ABSTRACT: Short sisal fiber (SF)-reinforced polypropylene (PP) composites were prepared by melt blending followed by injection molding. To improve the interfacial bonding between SF and PP, the PP matrix was maleated (MAPP) by blending PP and maleic–anhydride-grafted-PP in the weight ratio of 9/1. It was found that the SF/MAPP composites have lower melt viscosity (as reflected by torque rheometer measurements) than the SF/PP composites at the respective sisal fiber contents. In terms of mechanical properties, PP maleation has the effect of improving the tensile strength. This can be explained in terms of the improved SF/matrix interfacial bonding when MAPP was used. However, the impact strength was reduced when the PP matrix was maleated. The improved SF/matrix interfacial bonding prevented fracture mechanisms such fiber/matrix debonding and fiber pullout from taking place. © 2002 Wiley Periodicals, Inc. J Appl Polym Sci 85: 169–176, 2002

Key words: interfaces; poly(propylene) (PP); injection molding; composites

INTRODUCTION

Sisal fiber possesses good mechanical properties, and can be harvested from renewable resources. Recently, composites using sisal fiber as reinforcements have attracted considerable attention.[1,2] One of the key issues for sisal fiber composites is concerned with the weak fiber–matrix interface.[3–7] Silva and Al-Qureshi[3] have employed contact angle measurement and fiber pullout test to evaluate the effect of alkaline treatment on sisal fibers. Bisanda[4] studied the treatment of sisal fibers using sodium hydroxide solution. The treated sisal fiber/epoxy composites showed improvements in the compressive strength and water resistance. It was suggested that the removal of the intracrystalline and intercrystalline lignin and other surface waxy substances, by alkali, substantially increased the mechanical and chemical bonding.

Mishra et al.[5] have esterified a number of plant fibers, including sisal fiber with maleic anhydride (MA), for use as reinforcements in novolac resin. The MA reduced water and steam absorption to a great extent. The mechanical properties of the plant fiber/novolac composites were also increased with MA treatment. Thomas and coworkers have studied the effect of sisal fiber surface treatment for polyethylene[6] and polypropylene[7] matrix composites.

In this study, the injection moulding of sisal fiber-reinforced polypropylene will be investigated. The weak sisal fiber/PP interface issue will be improved by PP maleation, i.e., melt blending of maleic-anhydride-grafted-PP (MA-*g*-PP) with PP homopolymer. The resulting properties of the

Correspondence to: R. Li: (aprkyl@cityu.edu.hk).

Contract grant sponsor: the Research Grants Council of the Hong Kong Special Administrative Region, China; contract grant number: 9040422.

Journal of Applied Polymer Science, Vol. 85, 169–176 (2002)

maleated and nonmaleated composites will be evaluated and compared.

EXPERIMENTAL DETAILS

Polypropylene (PP, grade Pro-fax 6331, Montell) and maleic-anhydride-grafted-polypropylene (MA-*g*-PP, grade Epolene G-3003 WAX, Eastman Chemical) were used as the matrix and interface modifier respectively in this study. The sisal fiber used was obtained from a local supplier in the Guangdong Province of P.R. China. They were supplied as loose strands, and were alkali washed. The alkali treatment consisted of immersing the sisal fibers in a solution of 2% NaOH for 4 h at 60°C. Tensile properties of the treated sisal fibers are shown in Table I. To facilitate the melt compounding process, the supplied sisal fiber strands were cut into 10 mm lengths before melt blending with the matrix materials using the twin-screw extruder attachment for the Brabender Plasticorder. To improve the sisal fiber/matrix interfacial adhesion, the PP homopolymer was maleated, which was achieved by melt blending the PP and MA-*g*-PP pellets in the weight ratio of 9/1. The maleated PP/MA-*g*-PP blend will be designated as MAPP, while the PP homopolymer matrix will be simply designated as PP in this article. Due to the difficulties in melt blending and injection molding of the composites with too high sisal fiber content, the maximum sisal fiber content used in the study was 20 wt %. Summaries of the composites' composition and their designation are given in Table II.

The blended pellets were subsequently injection molded into ASTM type-I dumb bell-shaped tensile bars and rectangular plaques (80 × 150 × 3.3 mm) for tensile and Charpy impact tests, respectively. Tensile tests were carried out using a universal tensile tester (Instron model 4206). A clip-on extensometer was used to measure the tensile strain to give accurate measurement of the tensile Young's modulus. Charpy impact tests were carried out using a pendulum impact tester (Ceast). The impact specimens were pre-notched (notch-tip radius = 0.25 mm) with a notch cutter.

Table I Tensile Properties of the Sisal Fibers Used in This Study

Tensile Strength (MPa)	Tensile Modulus (GPa)	Elongation at Break (%)
495.6 [31.8]	12.9 [1.3]	3.8 [0.25]

Note: The standard deviations are shown in the square brackets [ ].

Table II Composition and Designation of Materials Used

	PP (wt %)	MA-*g*-PP (wt %)	Sisal Fiber (wt %)
PP	100	—	—
PP10	90	—	10
PP20	80	—	20
MAPP	90	10	—
MAPP10	81	9	10
MAPP20	72	8	20

To assess the melt processing characteristics of the sisal fiber-reinforced PP composites, 40 g of the respective composites were loaded into the internal mixer attachment of the Brabender Plasticorder and the torque was measured as a function of time. The measurements were carried out at 170°C and 50 rpm.

Thermal stability of the composites and the respective constituents were determined by thermal gravimetric analysis. Measurements were carried out using a thermal gravimetric analyzer (Seiko model SSC/5200) under pure helium and helium/oxygen (50/50 ratio) gas flow conditions. The weight loss against temperature was measured at a heating rate of 5°C/min.

Storage modulus and tan δ of the composites were measured by a dynamic mechanical analyser (TA Instruments model 2980). Measurements were carried out using the dual cantilever mode. The heating rate and frequency were 5°C/min and 0.5 Hz, respectively.

Fracture surfaces of the tested samples were examined by scanning electron microscopy (JEOL JSM 820). The fractured surfaces were coated with a thin layer of gold prior to SEM examination.

RESULTS AND DISCUSSIONS

The torque vs. blending time plots measured using the Brabender Plasticorder with the internal mixer attachment are shown in Figure 1. It can be seen that all the torque–time curves reached a high value of approximately 30 N-m within the

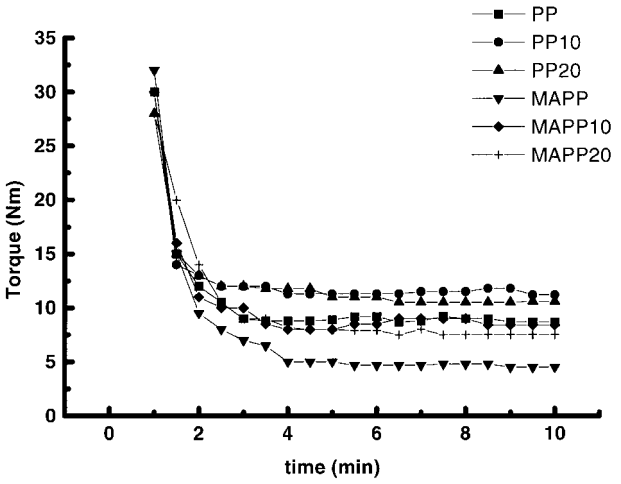

Figure 1 Torque vs. blending time plots for the sisal fiber-reinforced PP omposites.

first minute. This is due to the initial melting of the polymer matrix (i.e., PP or MAPP). Once the matrix has been completely melted, the torque reduced rapidly to the much lower steady state values, and remained constant up to over 10 min of blending time. The steady-state torque measured at the blending time of 10 min ($\tau_{10\text{min}}$) for the PP and MAPP matrices and their composites are shown in Figure 2. It can be seen that $\tau_{10\text{min}}$ for both matrices were initially increased with the addition of 10 wt % of sisal fibers, and decreased slightly when the fiber content was increased to 20 wt %. This is contrary to the results presented by Joseph et al.,[7] where $\tau_{10\text{min}}$ increased monotonically with increasing sisal fiber content. A possible reason was that the starting sisal fiber lengths ranged from 2 to 30 mm before melt blending in ref. 7. Our starting fiber lengths were all close to 10 mm.

Furthermore, by referring to Figures 1 and 2, $\tau_{10\text{min}}$ was significantly lower for the MAPP system irrespective of whether sisal fibers were incorporated or not. $\tau_{10\text{min}}$ for both MAPP10 and MAPP20 are lower than that for the PP homopolymer. The MA-*g*-PP can therefore function as processing aid in both melt compounding and injection molding of the composites.

The stability of the sisal fibers under the high melt processing temperature is of major concern. If serious degradation of the sisal fibers took place during melt processing of the composites, the mechanical reinforcement effects of the sisal fibers may be lost. Thermal gravimetric analysis (TGA) was employed to study the high temperature decomposition characteristics of the composites as well as the constituent phases. The thermal degradation behavior for PP and MAPP are shown in Figures 3(a) and 3(b), respectively. It can be seen that under the inert atmosphere (i.e., He), both PP and MAPP start to decompose at about 350°C, and the DTG curves have a peaks at just below 450°C. However, during melt compounding and injection molding, the PP melt will be in contact with trapped air. The thermal degradation behavior would be more appropriate to be investigated under oxygen containing conditions. In the presence of oxygen [i.e., the curves labeled $He+O_2$ in both Fig. 3(a) and (b)], the thermal degradation started at about 220°C, and the peak of the DTG (derivative of the TGA curve) curves occurred at about 280°C.

Thermal decomposition behavior for sisal fiber under He and $He+O_2$ atmosphere are shown in Figure 4. The decomposition of the sisal fiber in He atmosphere is a two stage process as indicated by the two peaks (~295 and 350°C, labeled as A and B, respectively) in the DTG curve. According to Albano et al.,[8] the first decomposition peak (A, 295°C) is due to the thermal depolymerization of hemicellulose and the glycosidic linkages of cellulose. The second decomposition peak (B, 350°C) is due to cellulose decomposition. The decomposition behavior is different when measured under the $He+O_2$ atmosphere. The two decomposition processes (which are labeled A* and B* to identify with the two processes A and B, respectively) were both reduced in the presence of oxygen. It is believed that the two processes A* and B* are

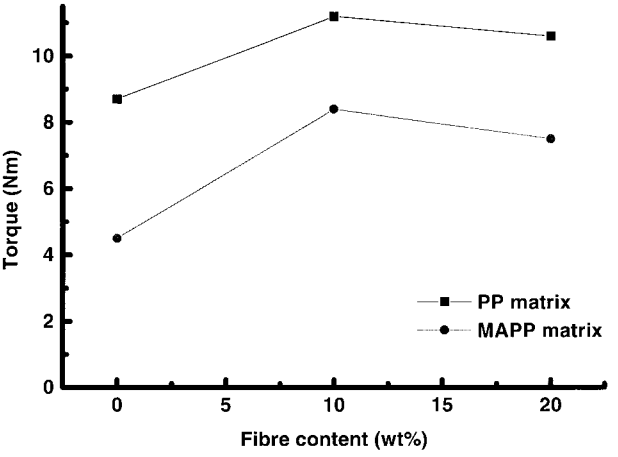

Figure 2 Steady-state torque vs. sisal fiber content for the composites measured at the blending time of 10 min.

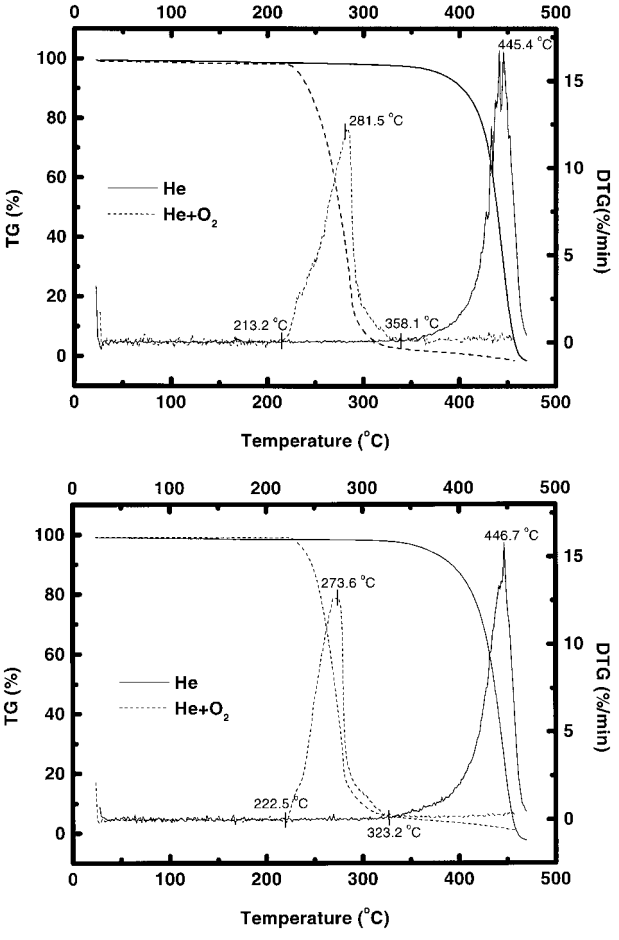

Figure 3 TGA and DTG curves measured under He and $He+O_2$ atmosphere for (a) PP and (b) MAPP.

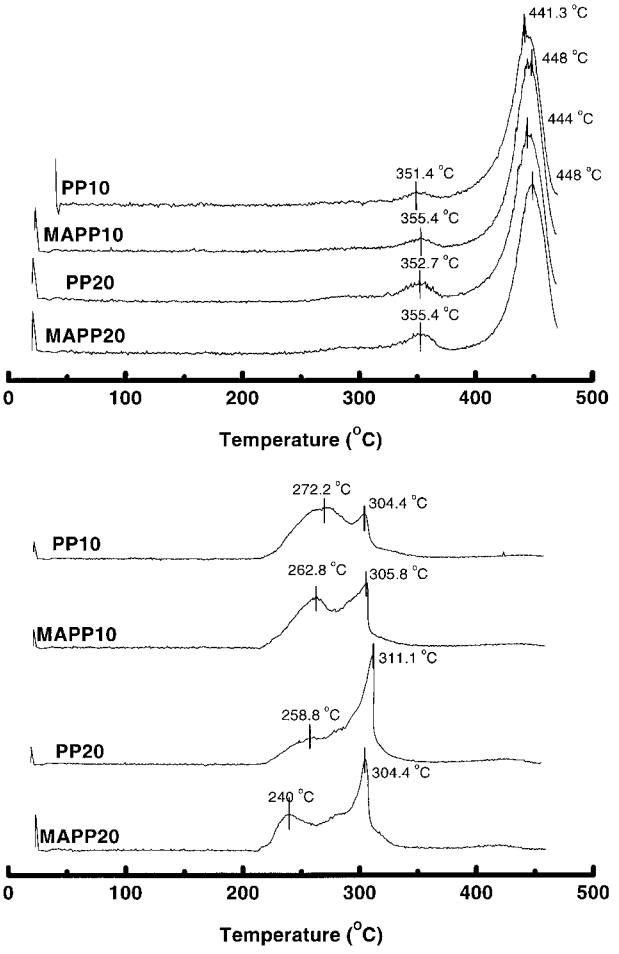

Figure 5 DTG curves for the SF/PP composites measured under: (a) He; and (b) $He+O_2$.

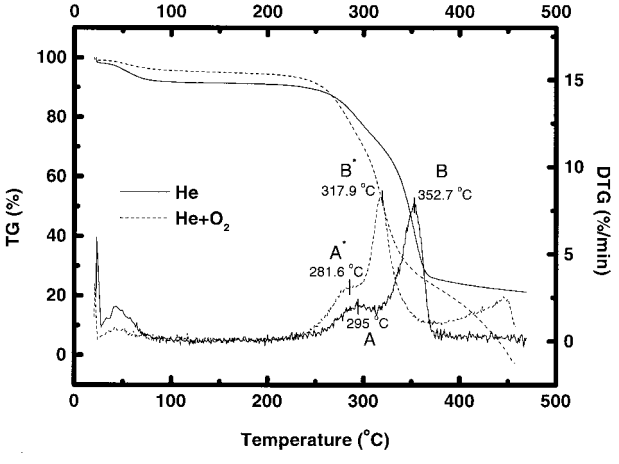

Figure 4 TGA and DTG curves for sisal fiber measured under He and $He+O_2$ atmosphere.

similar in nature to the two processes A and B, but are both accelerated due to the presence of oxygen.

The DTG results for the composites measured under pure He condition are shown in Figure 5(a). By referring to Figure 4, the peaks of the stage A and stage B processes for sisal fiber occurred at 295 and 350°C, respectively. The stage A process can be barely detected in the PP20 and MAPP20 composites. Due to the lower sisal fiber content, it cannot be seen in the PP10 and MAPP10 composites. The stage B process, however, is very prominent in all the composites [the peaks around 350°C in Fig. 5(a)]. The peak at around 445°C for the composites is related to the decomposition of the PP (or MAPP) matrix. Under the He condition, decomposition of sisal fiber is completed before the decomposition of PP.

Under $He+O_2$ condition, decomposition of the composites started at ~215°C [Fig. 5(b)]. As the

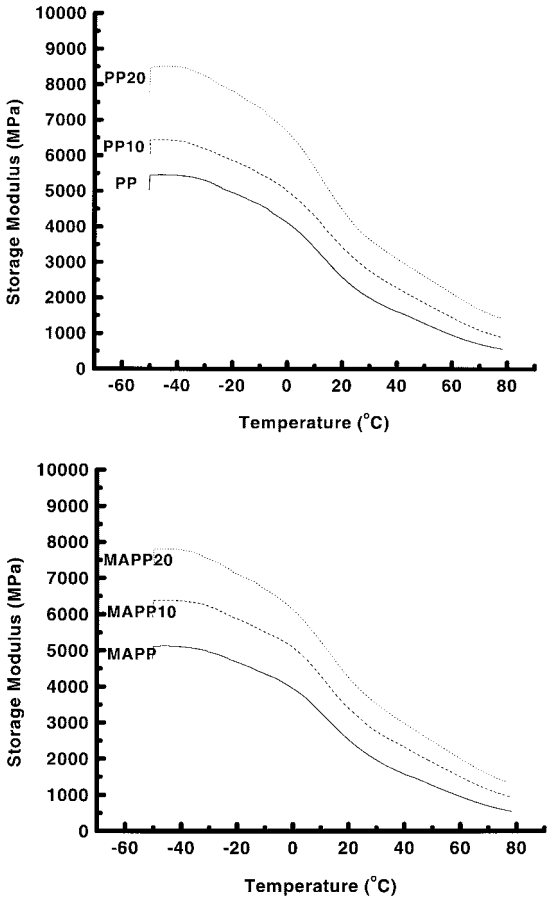

Figure 6 Plots of storage modulus (E') vs. temperature measured from DMA. (a) PP matrix composites; (b) MAPP matrix composites.

A* process for sisal fiber coincides with the decomposition of PP (compare Figs. 4 and 3), this gives rise to the broad (and sometimes undulating) initial peak(s). The final peaks at ~305°C correspond to the B* process for sisal fiber. In melt processing operations with the presence of oxygen, such as in extrusion or injection molding, the processing window that is suitable for polypropylene is also suitable for sisal fibers.

The storage modulus (E') vs. temperature plots for the PP and MAPP composites are shown in Figures 6(a) and 6(b), respectively. As expected, E' decreased with increasing temperature, with the most rapid reduction occurring around 10°C, which is the glass transition temperature (T_g) for PP [Fig. 6(a)]. Over the whole measurement temperature, E' increased with the increasing sisal fiber content. The tan δ vs. temperature plots measured around the T_g for PP are shown in Figure 7(a) and (b) for the PP and MAPP composites, respectively. It is obvious that T_g, as identified by the tan δ peak, was not much affected in the PP matrix composites, but was shifted to lower temperature in the MAPP composites. The reduction in T_g is related to the stronger interfacial bonding between MAPP and sisal fibers.

Typical tensile load–elongation curves for the PP and MAPP composites are shown in Figure 8. For both unreinforced matrices (i.e., PP and MAPP), they exhibit ductile behavior, that is, yielding occurred at the load maximum followed by cold drawing of the neck. With the addition of sisal fibers, the tensile characteristics changed to semibrittle. The variation of the Young's modulus with sisal fiber content is shown in Figure 9(a), and it can be seen that it is not much affected by PP maleation. This is consistent with the storage modulus (E') measurements (see Fig. 6). When one looks at the tensile strength, the effect of sisal fiber is different for the PP and MAPP composites [Fig. 9(b)]. For the PP matrix composites, the

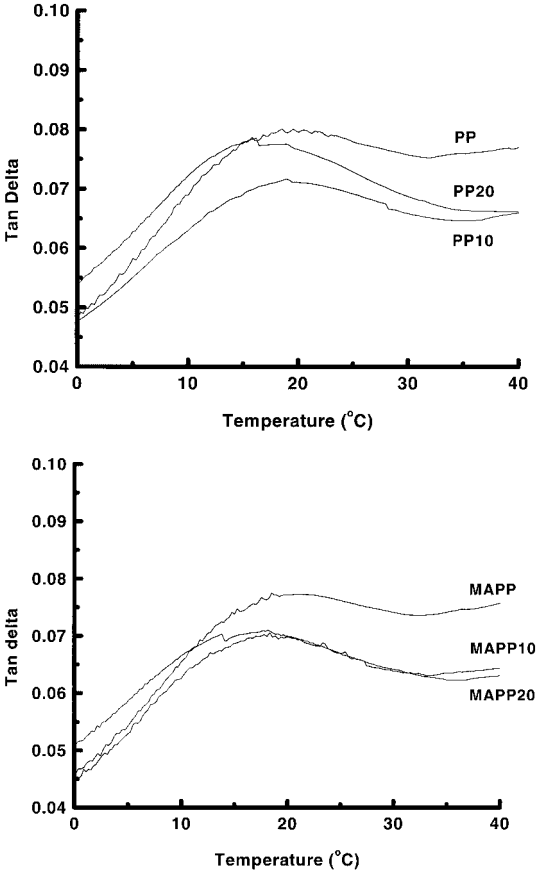

Figure 7 Plots of tan δ vs. temperature measured from DMA: (a) PP matrix composites, (b) MAPP matrix composites.

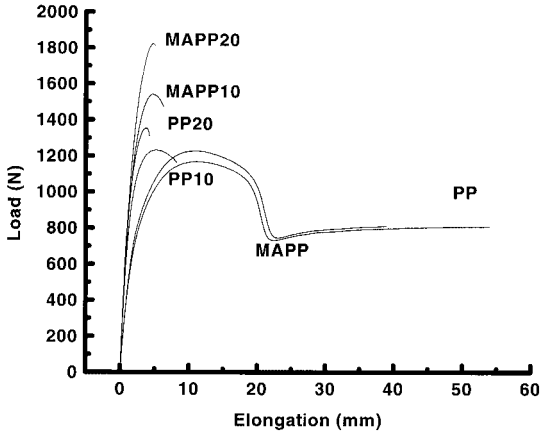

Figure 8 Tensile load–elongation curves for the PP and MAPP composites.

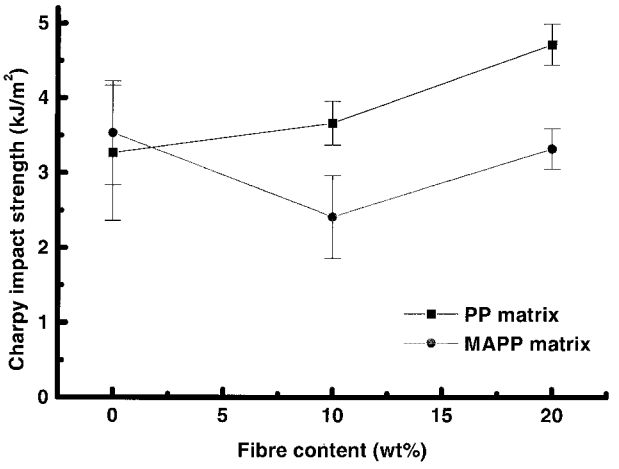

Figure 10 Effect of sisal fiber content on the Charpy impact strength of PP and MAPP composites.

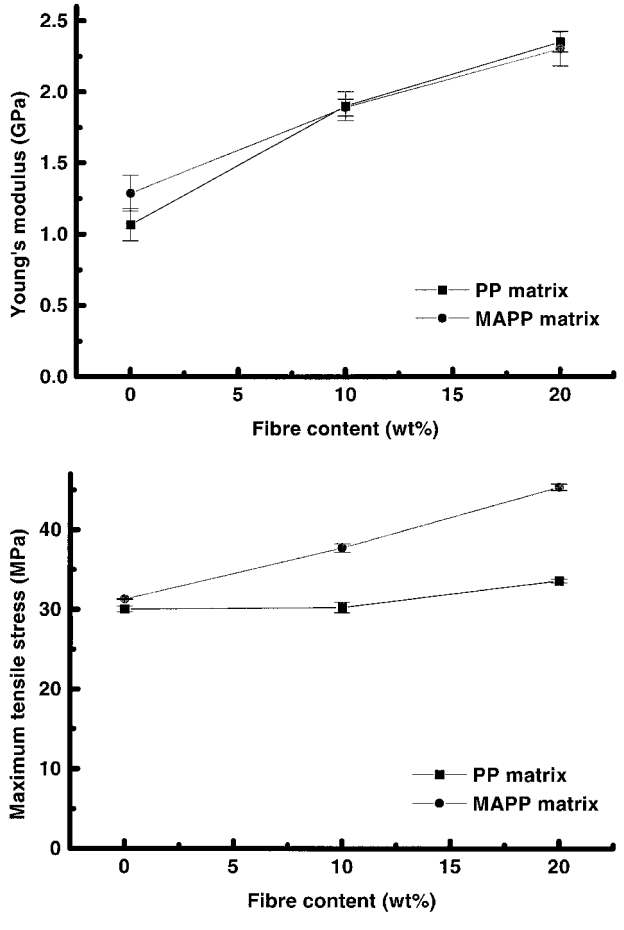

Figure 9 Effect of sisal fiber content on the tensile behavior of PP and MAPP composites: (a) Young's modulus; (b) Tensile strength.

tensile strength is not much affected by increasing sisal fiber content. For the MAPP matrix composites, the improvement of tensile strength with sisal fiber is significant. For both 10 and 20 wt % sisal fiber contents, the composites with MAPP matrix have higher tensile strength than that with PP matrix. This is due to the improved interfacial fiber/matrix bond strength when PP is maleated, as supported by the lowered T_g in the MAPP composites [Fig. 7(b)]. The improved interfacial bond strength allows more effective load transfer to the load-bearing sisal fibers.

The improved fiber/matrix interfacial bond strength, however, has a negative effect on the Charpy impact strength (Fig. 10). For the PP matrix composites, the impact strength increased with sisal fiber content. However, for the MAPP composites, the impact strength was reduced after the sisal fibers were introduced. To explain the toughening behavior difference for the two types of composites, SEM examinations were conducted to elucidate the energy absorption mechanisms such as fiber matrix debonding and fiber pull-out. Figure 11(a) shows the impact fracture surface for a PP20 composite at $\times 50$ magnifications, from which lots of pull-out fibers can be seen. The pull-out fibers fall into two size ranges: the bigger fibers have diameters around 100 μm, and the smaller fibers have diameters around 10 μm. It is known that a sisals fiber consists of bundles of tubular microfibers of 4–12 μm diameter. The cell wall of a tubular microfiber is 1–2 μm thick, and has a composite structure of lignocellulosic material reinforced by helical microfibrillar bands of cellulose. The cell walls are, in

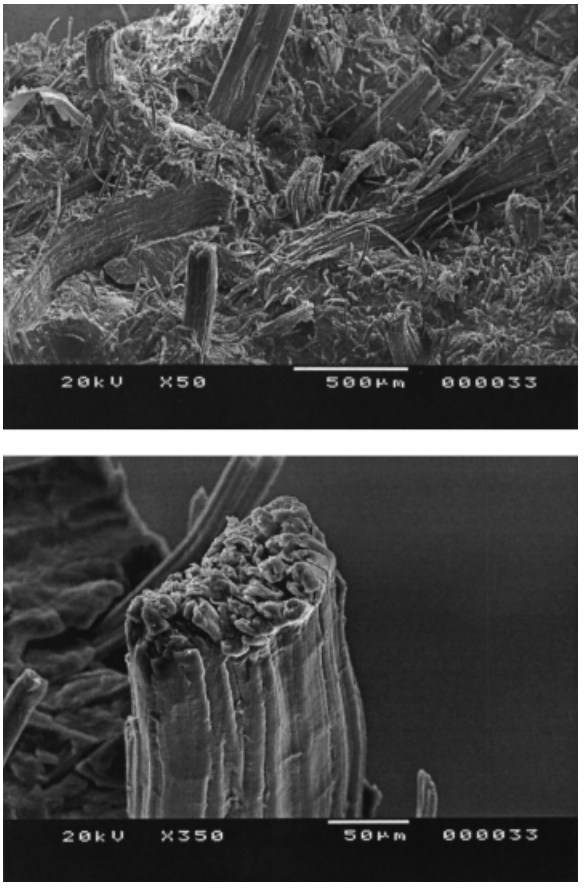

Figure 11 SEM fractographs showing the impact fracture surface for a PP20 specimen. (a) 50 × magnification. (b) 350 × magnification.

turn, covered by a layer of bonding material that separates one microfiber from another.[9–11] The smaller fibers (diam. ~10 μm) in Figure 11(a) are, therefore, the tubular microfibers, which were torn away from the main sisal fiber bundles during melt processing. Figure 11(b) shows a pull-out sisal fiber bundle from the PP20 specimen, where the individual tubular microfiber ends can still be identified. The fiber bundle surface is clean and without any PP adhesion. The energy absorption mechanisms for the nonmaleated PP composites therefore consist of: (1) fiber/matrix debonding, which may not be very significant as the bond strength is weak; and (2) fiber pull-out.

The impact fracture surface for MAPP20 and MAPP10 specimens are shown in Figure 12(a) and (b), respectively. In sharp contrast to the PP20 specimen [Fig. 11(a)], fiber pull-out in the MAPP20 specimen was suppressed. At a low magnification [×50, Figure 12(a) and (b)], the fracture surface is relatively flat. Figure 12(c) shows a small pultruded sisal fiber bundle for the MAPP10 specimen. The fiber now had a short pull-out length, and was well covered by the mal-

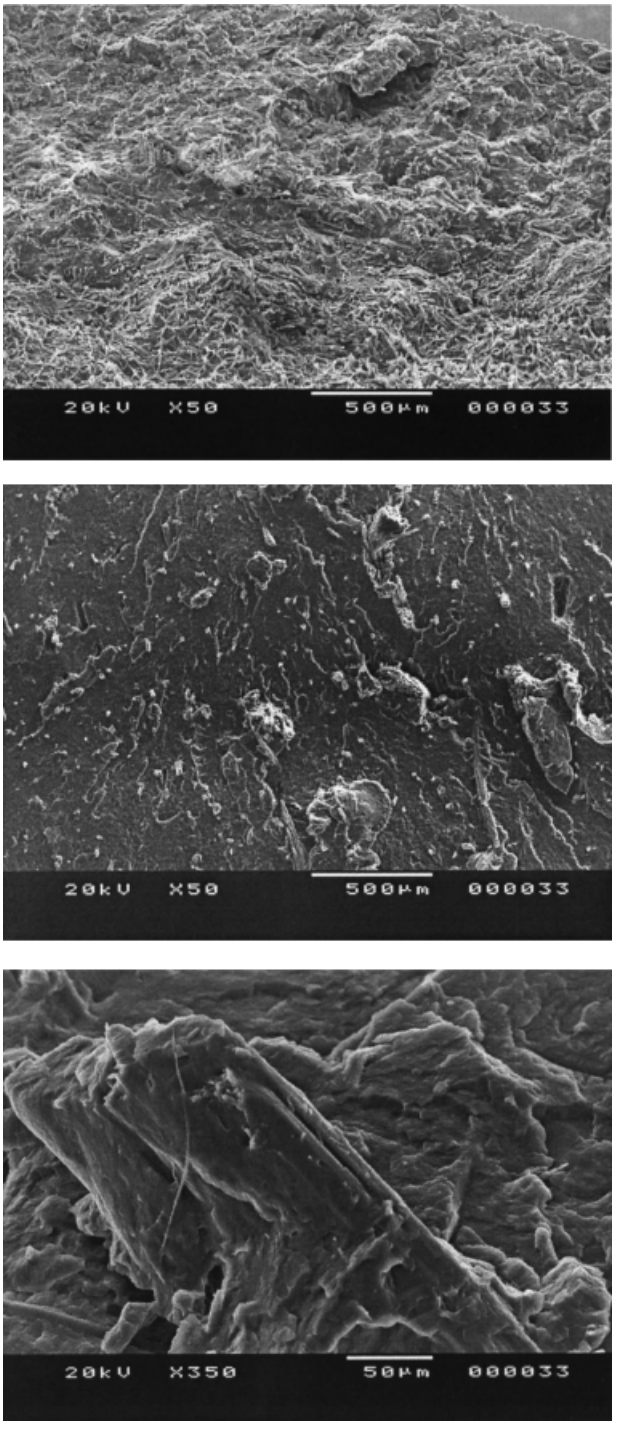

Figure 12 SEM fractographs showing the impact fracture surface for SF/MAPP composites. (a) MAPP20 at 50 × magnification; (b) MAPP10 at 50 × magnification; (c) MAPP10 at 350 × magnification.

eated PP. The individual tubular microfiber ends cannot be seen, as they were also covered by the MAPP. For the maleated specimens, both fiber/matrix debonding and fiber pull-out were limited. The energy absorption mechanisms in the SF/MAPP composites consisted of matrix and fiber fracture only.

CONCLUSIONS

The effect of matrix maleation and fiber content on the processability, mechanical properties, and morphology of sisal fiber (SF)-reinforced polypropylene composites were investigated. Maleated PP and its SF composites have lower melt viscosities than the corresponding counterparts as indicated by torque-rheometer measurements. Sisal fibers can function as reinforcements, as both the tensile modulus and tensile strength were improved with increasing sisal fiber content. While PP maleation has no effect on the tensile modulus, the tensile strengths of the composites were significantly improved when MAPP was used instead of PP. This can be explained by the much improved fiber/matrix interfacial bonding in the SF/MAPP composites. The impact strength, however, was reduced for the stronger fiber/matrix interfacial bonding in the SF/MAPP composites.

The work described in this article was supported by a grant from the Research Grants Council of the Hong Kong Special Administrative Region, China (Project No. 9040422).

REFERENCES

1. Bledzki, A. K.; Gassan, J. Prog Polym Sci 1999, 24, 221.
2. Li, Y.; Mai, Y. W.; Ye, L. Comp Sci Technol 2000, 60, 2037.
3. Silva, J. L. G.; Al-Qureshi, H. A. J Mater Process Technol 1999, 92–93 124.
4. Bisanda, E. T. N. Appl Compos Mater 2000, 7, 331.
5. Mishra, S.; Naik, J. B.; Patil, Y. P. Comp Sci Technol 2000, 60, 1729.
6. Joseph, K.; Thomas, S.; Pavithran, C. Polymer 1996, 37, 5139.
7. Joseph, P. K.; Joseph, K.; Thomas, S. Comp Sci Technol 1999, 59, 1625.
8. Albano, C.; González, J.; Ichazo, M.; Kaiser, D. Polym Degrad Stabil 1999, 66, 179.
9. Bisanda, E. T. N.; Ansell, M. P. J Mater Sci 1992, 27, 1690.
10. Bai, S. L.; Wu, C. M. L.; Li, R. K. Y.; Zeng, H. M.; Mai, Y. W. Adv Compos Lett 1999, 8, 13.
11. Tsang, F. F. Y.; Jin, Y. Z.; Yu, K. N.; Wu, C. M. L.; Li, R. K. Y. J Mater Sci Lett 2000, 19, 1155.